EUROPEAN ORGANIZATION FOR NUCLEAR RESEARCH

CERN/EP 80-17
11 February 1980

DIFFRACTION DISSOCIATION, RESONANCES AND DECK MECHANISM IN THE Kω SYSTEMS OF THE REACTIONS $K^{\pm}p \to (K^{\pm}\omega)p$

Aachen-Berlin-CERN-London-Vienna Collaboration

and

Birmingham-Brussels-CERN-Mons-Serpukhov Collaboration

G. Otter, G. Rudolph and H. Wieczorek
III. Physikalisches Institut der RWTH, Aachen

J.J. Schreiber and R. Klein
Institut für Hochenergiephysik der Akademie der Wissenschaften der DDR, Berlin-Zeuthen

G.T. Jones, J.B. Kinson and K.M. Storr
University of Birmingham, Physics Department, Birmingham

D. Johnson
Inter-University Institute for High Energies, ULB-VUB, Brussels

V.T. Cocconi, Y. Goldschmidt-Clermont, G. Grammatikakis*, D.R.O. Morrison, H. Saarikko**, P. Schmid, A. Stergiou*** and J. Tuominiemi+
CERN, European Organization for Nuclear Research, Geneva

K.W.J. Barnham and B. Pollock++
Blackett laboratory, Imperial College of Science and Technology, London

R. Windmolders and P. Herquet
Faculté des Sciences, Université de L'Etat, Mons

B. Buschbeck and J.N. MacNaughton
Institut für Hochenergiephysik der Österrreichischen Akademie der Wissenschaften, Vienna

Submitted to Nucl. Phys. B

---

* Now at Nucl. Res. Centre Democritos, Athens, Greece.

** Now at Phys. Inst. Univ. Bonn, Germany.

*** Now at Inst. of Theor. Physics. Univ. of Nijmegen, Holland.

\+ Now at Helsinki Univ., Finland.

++ Now at Westfield College, London, U.K.

VTC/cg

ABSTRACT

A study is presented of the reactions $K^+p \to (K^+\omega)p$ at 8.25 and 16 GeV/c and $K^-p \to (K^-\omega)p$ at 10 and 16 GeV/c. The $(K^+\omega)$ and $(K^-\omega)$ mass spectra both present a strong enhancement very near threshold, while a second peak at $\sim$ 1.7 GeV is evident only with incident K^-. The threshold peak has very weak energy dependence and is mostly due to the 1^+S state which is produced conserving s-channel helicity. As these properties are the same as known for the $K\rho$ decay system of the diffractively produced 1^+ resonance $Q_1(1290)$, it is suggested that the $(K\omega)$ is another decay mode of that resonance. The ratio of the Q_1 coupling constants to the $K\omega$ and $K\rho$ decay channels, $R_\omega = g^2_{K\omega}/g^2_{K\rho}$ is determined to be 0.21 ± 0.04. For $(K\omega)$ masses above 1.4 GeV, the production cross section decreases rapidly with increasing energy, suggesting Reggeon exchanges. The enhancement at 1.7 GeV is predominantly, but not exclusively, due to the 2^- state, which is found to be 1.5 times stronger in K^- than in K^+ reactions. The favoured production of $(K^-\omega)$ over $(K^+\omega)$ is explained in the framework of the Deck model by the fact that in K exchange processes, the virtual K^-p scattering, non-exotic, is favoured over the exotic K^+p scattering.

1. INTRODUCTION

Diffraction dissociation of the incoming kaon in Kp scattering has recently been shown to have rich internal structure. A 1^+ resonance at a mass of $\sim$ 1290 MeV, Q_1, mainly decaying into Kρ, has been established by partial wave analysis of the (K$\pi\pi$) system [1,2] and two more resonances with $J^P = 1^+$ ($Q_2(1400)$) and 0^-, respectively, have been claimed [2,3] in the Q region (1.2 - 1.4 GeV). Less is known about the nature of the second enhancement in the (K$\pi\pi$) mass spectrum - the L region (1.6 - 1.9 GeV). Its cross section, mass shape and resonance content were found to be different in K^+p and K^-p scattering [4].

Important additional information about diffractively produced resonances and the production mechanisms involved can be obtained from a study of low mass (Kω) systems in the reaction

$$Kp \rightarrow (K\omega)p \quad . \tag{1}$$

Compared to the (K$\pi\pi$) system which contains several resonant substates $K^*(890)$, $K^*(1420)$, κ, ρ, f and ε), the (Kω) system is simple.

Reaction (1) has been studied at several energies both in K^+p and in K^-p interactions [5-8]. With incident K^+ at 10 and 12 GeV/c, a strong broad threshold enhancement was observed, but no distinct state could be resolved in the L region. On the other hand, a (Kω) decay mode of the L was observed in K^-p interactions at 10 GeV/c [6]. Significant structure in the mass spectrum and in the moments of the (Kω) angular distribution were found in K^-p interactions at 7.3 GeV/c [7]. There and in another publication on K^-p data at 10 and 16 GeV/c [8], the production of the 1^+S (Kω) state near threshold was found to be close to s channel helicity conservation. A possible relation of this result to the 1^+S (Kρ) state at the same mass has been discussed in ref. [9].

In this work we intend to re-investigate the (Kω) system in reaction (1) with increased statistics and to compare systematically the K^+ and K^- induced reactions. To do this, we use data from four bubble chamber experiments, two K^+p experiments at 8.25 and 16 GeV/c and two K^-p experiments at 10 and 16 GeV/c.

The data selection is described in sect. 2. Sect. 3 presents the experimental results on the ($K\omega$) mass spectra, cross sections, momentum transfer and angular distributions. The partial wave content of the ($K\omega$) system, determined by maximum likelihood fits, is described in sect. 4. Sect. 5 contains a discussion of the results and sect. 6 summarizes the conclusions.

2. DATA SELECTION

The four-prong events of K^+ interactions at 8.25 and 16 GeV/c, and of K^-p interactions at 10 and 16 GeV/c, observed in the CERN 2m hydrogen bubble chamber, were measured, reconstructed and fitted to the hypothesis

$$K^{\pm}p \to K^{\pm}\pi^+\pi^-\pi^0 p. \qquad (2)$$

Details of the selection procedure based on fit probabilities and missing mass of the neutral system have been described elsewhere [8,10].

The number of events found in the four experiments are listed in table 1.

Many of the fits to reaction (2) are ambiguous with other hypotheses, as ambiguities of $K^{\pm}$ with $\pi^{\pm}$, of p with π^+ and of π^0 with K^0 or neutrons often cannot be resolved by kinematic fitting. However, the problem of ambiguities is greatly reduced and becomes, in practice, unimportant for the subset of events that we consider in this work, namely those corresponding to the reaction (1), $Kp \to (K\omega)p$, where the ($K\omega$) system has invariant mass smaller than 2 GeV. First of all, because of the small 4-momentum transfers observed, the small ($K\omega$) mass implies that the proton has low momentum, and hence is recognizable by ionisation. Furthermore, requiring that the three pions have effective mass in the ω meson band and attributing weight one to all hypotheses fitting reaction (2) guaranties that no true event of reaction (1) is lost and relegates possible false hypotheses to lie in the background.

With the selection

$$0.76 < M(\pi^+\pi^-\pi^0) < 0.81 \text{ GeV} \quad , \qquad (3)$$

the ω signal to background ratio is found to vary from 6 close to the $(K3\pi)$ threshold to about 3 at $(K3\pi)$ masses of $\approx$ 2 GeV. The number of events with $M(K3\pi) < 2$ GeV and satisfying condition (3) are also listed in table 1. In the following, these two conditions will be used to define the event sample for reaction (1). Comparing this sample with events having $M(3\pi)$ outside the ω mass band, we have verified that background effects are in general smaller than the statistical errors.

3. EXPERIMENTAL RESULTS

3.1 $(K\omega)$ mass distributions

In fig. 1 we show the $(K\omega)$ mass distributions of our four experiments, together with the spectra obtained in 7.3 GeV/c K^-p [7] and 10 GeV/c K^+p interactions [5]. At all energies the production cross section is large close to threshold. As in the spectrum at 7.3 GeV/c, a clear second maximum at around 1.7 GeV is seen in K^-p interactions at 10 GeV/c, which is reduced to a pronounced shoulder at 16 GeV/c. In K^+p reactions there are indications of a shoulder around 1.7 GeV at all three energies shown, but, as at 12 GeV/c [5], no clear enhancement is seen.

The differences between K^+ and K^- induced reactions become more obvious when the sample of events is split into two subsets according to the sign of $\cos\theta_{GJ}(\omega)$, the Gottfried-Jackson angle of the ω in the $(K\omega)$ rest frame. The mass spectra for the positive and negative values of $\cos\theta_{GJ}(\omega)$ are shown in fig. 2 for the K^+ and K^- experiments. When events with $\cos\theta_{GJ}(\omega) < 0$ are selected, the spectra for K^+p and K^-p experiments look similar and have only one broad threshold maximum. For $\cos\theta_{GJ}(\omega) > 0$ a narrow spike close to threshold is seen for both K^+ and K^-. With increasing mass, the spectra look quite different, however. Whereas an enhancement peaking around 1.6 GeV is seen for K^+p, a relatively narrow structure peaking at 1.7 GeV appears for K^-p. These differences between K^+p and K^-p data are also observed when comparing only the lower energy spectra (8.25 GeV/c K^+p and 10 GeV/c K^-p) or only the spectra at the higher energies (16 GeV/c $K^{\pm}p$).

3.2 Energy dependence of the (Kπ) production cross section

Information about the production mechanisms involved can be obtained from the energy dependence of the production cross section. To determine the (Kω) production cross section, the mass of the (3π) system was plotted in several intervals of the (K3π) mass and in each interval the number of omegas were determined by subtracting a hand-drawn background. The results and the topological microbarn equivalents used are listed in table 1. The errors given are the combination of the statistical error with a 5 to 10% systematic error accounting for the uncertainty in the background substraction and in the microbarn equivalent.

Fig. 3 plots our cross sections as functions of p_{LAB}, together with those obtained in the 10 and 12 GeV/c K^+p experiments and in the K^-p experiment at 7.3 GeV/c.

These data have been fitted with the function

$$\sigma = C\, p_{lab}^{-n} \qquad (4)$$

and the results for the exponent n are shown in fig. 4. The n values in K^+p reactions are found to be consistently larger than in K^-p. The increase of n with (Kω) mass is similar, however. The small energy dependence close to threshold indicates a strong diffractive component in the production of low mass (Kω) systems, especially in the K^-p case. In the L region n is $\sim$ 1, showing that non-diffractive mechanisms contribute substantially in the energy range considered. The different energy dependence for the low and high mass (Kω) systems is clearly seen in the change with energy of the relative strength of the two enhancements in K^-p reactions (fig. 1).

3.3 Momentum transfer distributions

In fig. 5 the distributions in $t' = |t_{pp} - t_{min}|$ of the events of reaction (1) are presented for four (Kω) mass intervals, combining data of all our four experiments. This combining of K^+p and K^-p data is justified by the fact that, within our limited statistics, no significant differences in the t' distributions between K^+p and K^-p reactions or among the different energies could be observed.

The t' distributions have been fitted with a simple exponential (excluding the point in the first t' bin, 0 - 0.05 GeV^2). The values obtained

for the slopes, reported in the figure, range from 7.2 ± 0.5 GeV^{-2} at (Kω) masses below 1.4 GeV, to 5.3 ± 0.6 GeV^{-2} for M(Kω) = 1.8 - 2.0 GeV. These values are similar to those reported for the (Kρ) system in the reaction $K^- p \to (K^- \rho^0)p$, and are smaller than those obtained for the (K$\pi\pi$) system of reaction (2), where the slopes vary from ~ 9 GeV^{-2} near the (K$\pi\pi$) threshold, to ~ 7 GeV^{-2} for (K$\pi\pi$) masses in the 1.8 - 2.0 GeV interval [9].

3.4 Moments of the (Kω) angular distribution

To study the internal angular structure of the (Kω) system and to take into account information on the polarization of the ω derived from its decay distribution, we calculate the double moments in the Gottfried-Jackson frame

$$H(LM,\ell m) = \langle D^{L}_{Mm}\ (\Phi,\ \Theta,\ 0)\ .\ D^{\ell}_{m0}\ (\phi,\ \theta,\ 0)\rangle \quad . \tag{5}$$

Φ and Θ are the azimuthal and polar angles of the ω in the (Kω) rest frame; ϕ and θ are the angles of the normal to the decay plane measured in the ω helicity frame with the standard choice of axes [11]. The moments H(LM,00) with $\ell = m = 0$ are proportional to $\langle Y^{L}_{M}\ (\cos\Theta,\ \Phi)\rangle$, the moments of the spherical harmonics.

In fig. 6 we show the most significant normalized moments as functions of the (Kω) mass for $K^+ p$ and $K^- p$ data (combined in energy). Specially interesting is the moment H(10,00) which simply measures the forward-backward asymmetry in the Gottfried-Jackson system. This asymmetry is related in an obvious way to the shape of the mass spectra shown in fig. 2. At low (Kω) masses we find the asymmetry characteristic of many diffractively produced systems: forward going kaons are preferred over backward going ones. This asymmetry changes sign at (Kω) mass of ~ 1.6 GeV and flips back at higher masses. This is true for both $K^+ p$ and $K^- p$ data, although the exact position of the change in sign may be different for the two cases.

H(20,00) is strongly positive throughout the mass region considered and also H(30,00) seems different from zero. Moments with $L > 4$ are compatible with zero up to ~ 2 GeV. We conclude that spin states with at least $J = 2$ are present in the (Kω) system below 2 GeV. Moments with $M = 1$ are also found to be different from zero, e.g. H(11,00) and H(21,00), indicating the presence of states with t channel helicity 1.

The moment H(00,20) is related to the helicity λ of the ω in the (Kω) rest frame. In fact, the combinations

$$\Sigma_0 = \frac{1}{3}\,[H(00,00) + 5\,H(00,20)]$$
$$\text{and} \qquad \Sigma_1 = \frac{2}{3}\,[H(00,00) - \frac{5}{2}\,H(00,20)] \qquad (6)$$

measure the amount of ω's with helicity 0 and 1, respectively (the sum $\Sigma_0 + \Sigma_1 = H(00,00)$ is 1 for normalized moments or equal to the number of events for unnormalized ones). The unnormalized combinations Σ_0 and Σ_1 are shown in fig. 7. For the K^-p experiment, Σ_0 is largest at low masses and does not show an enhancement in the L region, which, however, is clearly seen in Σ_1. As already observed by Chung et al. [7], this result seems to indicate that the L enhancement is mainly related to helicities $\lambda = 1$. In K^+p, however, the situation is less clear.

4. PARTIAL WAVE ANALYSIS

A modified version of the Illinois partial wave analysis program [12] was used to determine the partial wave content of the (Kω) system in given mass intervals, integrated over t' from 0 to 0.8 GeV^2. The states are labelled by J^P LMη, where J^P denote spin and parity of the state, L the relative angular momentum between K and ω, M the spin projection onto the z axis (either of the Gottfried-Jackson or of the s channel helicity frame) and η the naturality of the t channel exchange [13]. To increase statistics we have always combined the data at different energies.

The analysis consists of three parts:

(i) First we reinvestigate (Kω) systems at very low masses, namely from threshold up to 1.35 GeV. In this mass interval we find 110 events for the combined K^+ experiments and 113 events for the K^- experiments. The states 0^- P0+, 1^+ S0+ and 1^+ S1+ are sufficient to describe the data. Fits were done both in the s and t channel helicity frames and gave consistent results. The number of events assigned to 0^- and 1^+ and the density matrices of the 1^+S state in both frames are presented in table 2. For

K^-p, excellent agreement with s channel helicity conservation is found (ρ_{11+} and Re ρ_{01+} consistent with zero in the helicity frame), confirming previous results. For K^+p, the situation is less simple: the element ρ_{00} deviates from unity by 2-standard deviations, while Re ρ_{01+} is consistent with 0 in the s channel, but not in the t-channel helicity frame.

(ii) Next we present results of fits to $(K^+\omega)$ and $(K^-\omega)$ data in several mass intervals from 1.3 to 2.0 GeV. With increasing $(K\omega)$ mass, higher partial waves start to contribute and the number of possible states becomes large. Because of limited statistics we are unable to decide on the contributions of states at the 10-15% level in individual mass intervals. Therefore, we try to find a minimum set of states which describes the data reasonably well in consecutive mass intervals. With such a requirement we can study the mass dependence of the dominating states, but we are not sensitive to narrow states which contribute less than $\sim$ 15% in a single mass interval.

To fit $(K^+\omega)$ and $(K^-\omega)$ data separately, we chose overlapping intervals of the $(K\omega)$ mass, 200 MeV wide, in steps of 100 MeV. The results are presented in table 3 together with the number of events in each bin. For masses below $\sim$ 1.6 GeV, the states 0^-P0+, 1^+S0+, 1^+S1+, 2^+D1+, 2^+D0- were found sufficient to describe the data. A remarkable difference between $(K^+\omega)$ and $(K^-\omega)$ data is found for the states 0^-P0+ and 1^+S1+. In the mass interval 1.4 - 1.6 GeV, a much stronger contribution of 1^+S1+ and less 0^-P0 are required for $(K^-\omega)$ than for $(K^+\omega)$. This reflects the difference in the moment H(11,00) which is strongly positive in $(K^-\omega)$, but compatible with 0 in $(K^+\omega)$. A possible interpretation of this difference will be presented in sect. 5.

For masses of the $(K\omega)$ system above 1.6 GeV, the contributions of the states 0^-P and 1^+S are much smaller than at lower masses. For both $(K^+\omega)$ and $(K^-\omega)$, a substantial amount of 2^-0 was found and the fits improved significantly by including both P and F waves. However, the amount of 2^- is $\sim$ 1.5 times stronger in $(K^-\omega)$ than in $(K^+\omega)$, which may be related to the fact that a peak in the mass distribution in the L-region is better seen with K^- than with K^+. The 2^- states with helicity 1 were tried and gave some contribution, but well below the 15% level. The states with J = 3 account

for background of higher spin. The state 3^-F improved the fits in the highest mass interval (1.8 - 2.0 GeV); 3^+D was found to be present in $(K^+\omega)$, but not in $(K^-\omega)$. However, with the present statistics, we prefer to consider these states as background parametrization rather than interpret them as physical states. The goodness of the fits was studied by generating Monte-Carlo events according to the fit results, calculating moments $H(LM,\ell m)$ for these samples and comparing them to the moments obtained from the experimental data. The calculated moments are indicated by crosses in fig. 6. Most of the moments are reasonably well described by the fit. The worst disagreement is for $H(10,21)$ in K^+p, where the fit cannot reproduce the values different from zero found experimentally. For $H(11,00)$ in K^-p, the Monte-Carlo results have the correct trend, but cannot fully account for the experimental values.

(iii) Finally, in order to study the mass dependence of the partial waves in more detail, $(K^+\omega)$ and $(K^-\omega)$ data were combined, and fits were done in 100 MeV intervals from threshold up to 2 GeV. Combining K^+ and K^- data seems justified by the approximate similarity of the moments and of the fit results for $(K^+\omega)$ and $(K^-\omega)$. The existing differences, specially in the 1.4-1.6 GeV region, will be averaged over, and interference terms will only have limited physical significance. The same set of states was used as for the fits in 200 MeV intervals (to account for background only 3^-F was included, 3^+D was omitted). The results found are consistent with the sum of those for $(K^+\omega)$ and $(K^-\omega)$ obtained previously in 200 MeV intervals. The overall mass distribution and the contributions of the individual J^P states are shown in fig. 8. The state 1^+S peaks at threshold and falls off smoothly with increasing mass. No evidence for an enhancement corresponding to $Q_2(1400)$ is seen. The state 0^-P has its maximum between 1.4 and 1.5 GeV and also decreases smoothly at higher mass. A broad structure between 1.6 and 1.9 GeV is observed for the state 2^- which is the dominating state and accounts for (35 ± 5)% of the events in this mass region.

5. DISCUSSION OF RESULTS

The production of $(K\omega)$ systems in reactions (1) has a strong threshold enhancement. The weak energy dependence of its production cross section suggests a substantial diffractive component. It has been observed previously [9] that the mass spectrum peaks much closer to threshold than

for diffractively produced $K^*\pi$ states and that in this it resembles the Kρ state. We confirm the similarity of the 1^+S (Kρ) and (Kω) states close to threshold, not only in the mass spectra but also in the production mechanism which is consistent with s channel helicity conservation.

The 1^+S (Kρ) state close to threshold has been interpreted as a resonance, Q_1, with mass M_0 = 1290 MeV and width Γ_0 = 150 MeV [14]. Because of the similarities between (Kρ) and (Kω) mentioned above, we assume the (Kω) threshold enhancement to be another decay mode of Q_1.

The cross sections for production of the state 1^+S ($K\rho^0$) with mass between 1.25 and 1.35 GeV and $|t'| < 0.8$ (GeV/c)^2 was found to be 17.3 ± 1.6 μb averaging results from an analysis of combined K^-p data at 10, 14.3 and 16 GeV/c beam momenta [1]. This value is consistent with 11.4 μb found for K^-p at 13 GeV/c [2] in the mass interval 1.24 - 1.34 GeV and $|t'| < 0.3$ (GeV/c)^2. In the same experiment, for K^+p, the cross section was found to be slightly higher (14.8 μb) in the same mass and t' regions.

For the production of the 1^+S (Kω) system we find 6.5 ± 0.8 μb for K^-p averaged over the 10 and 16 GeV/c data and 7.7 ± 1.2 μb for K^+p averaged over the 8.25 and 16 GeV/c data, again in the mass interval 1.28 to 1.35 GeV and for $|t'| < 0.8$ (GeV/c)^2. These values are obtained from the PWA results listed in table 2 after corrections for background and the Breit-Wigner tails of the ω. Uncertainties in the background subtraction are included in the error.

The fact that the central mass of Q_1 lies very close to the thresholds of the Kρ and Kω decay channels and the non-zero widths of ρ and ω make it difficult to determine relative branching ratios. As discussed by Dunwoodie and Lasinski [15], a more meaningful quantity to quote is the ratio of the coupling constant of Q_1 to the Kρ and Kω final states, $R_\omega = g^2_{K\omega}/g^2_{K\rho}$. Unlike the branching ratio, the ratio of coupling constants is rather independent of the exact knowledge of mass and width of the resonance. Using the method described in details in the Appendix, this ratio is found to be

$$R_\omega = g^2_{K\omega}/g^2_{K\rho} = 0.21 \pm 0.04 \quad . \tag{7}$$

The couplings of Q_1 and Q_2 to $K\omega$ are crucial parameters for correct SU(3) classification of these resonances and for an overall description of masses, widths and branching ratios of the members of the 1^+ multiplets [16,17]. In these classifications, the Q_1 and Q_2 are related to the multiplet members $Q_A(1^{++})$ and $Q_B(1^{+-})$ by a mixing angle θ_Q. Our final value of R_ω and our observation of a strong $K\omega$ signal below $M(K\omega) = 1.35$ GeV are consistent with the description of ref. [16] having, in particular, $\theta_Q = 41^0 \pm 4^0$. This description made use of our preliminary value of the branching ratio $(Q_1 \to K\omega)/(Q_1 \to K\rho^0)$. Our results contradict, however, a description proposed in ref. [17] with a much smaller value of θ_Q, in which the Q_1 should decouple from $K\omega$.

The similarity between $(K\omega)$ and $(K\rho)$ systems seems to hold not only at threshold for the state 1^+S, but also at higher masses. We can compare our results for $(K\omega)$ with the detailed results for $(K\rho)$ reported in refs [2,3] for $M(K\omega)$ up to $\sim$ 1.6 GeV. Differences between K^+p and K^-p data found for $(K\omega)$ production are also observed for $(K\rho)$. In both systems 1^+S1 appears to be stronger for K^-p than for K^+p around 1.5 GeV and, in the mass interval 1.5 - 1.6 GeV, 0^-P in K^+p is about twice as strong as in K^-p.

In sect. 3.2 we have related the marked difference in the states 1^+S1+ and 0^-P0+ for $(K^+\omega)$ and $(K^-\omega)$ systems to differences in the moments $H(11, 00)$, which in turn can be related to differences in the distributions of the azimuthal angle. Following a suggestion by E.L. Berger [18], we plot the event distributions in ϕ_s, the azimuthal angle of the ω in the s channel helicity system for $(K\omega)$ masses between 1.4 and 1.6 GeV (fig. 9). The differences between $(K^+\omega)$ and $(K^-\omega)$ are obvious. This angle ϕ_s, related to the momentum transfer from the incoming K to the ω, can be used to separate events according to different exchange mechanisms in a Deck model (fig. 9). With our conventions, events with $|\phi_s(\omega)| < 90^0$ will be produced mainly by ω exchange and events with $|\phi_s(\omega)| > 90^0$ mainly by K exchange. Indeed, for $|\phi_s(\omega)| > 90^0$ the cross section is larger for virtual K^-p scattering, which is non-exotic, than for K^+p scattering, which is exotic. As in other reactions [19], the Deck model thus provides at least a qualitative interpretation of the data. The model would predict also differences for K^+ and K^- exchanges in the slope of the $d\sigma/dt'$ distributions, but our samples are too small to allow such a test.

The relatively large amount of 0^-P in the (Kω) mass interval 1.4 to 1.6 GeV found by partial wave analysis is consistent with the fact that the momentum transfer distribution in this mass interval does not show any indication of flattening near t' = 0 (see fig. 4). The 0^- states are in fact known to have steeply falling t' distributions [1-3] which compensate the flattening caused by helicity flip amplitudes.

Significant differences between $(K^+\omega)$ and $(K^-\omega)$ data are also present in the L region. A clear peak is seen in $(K^-\omega)$ mass spectra, mainly when selecting events with $\cos\theta_J(\omega) > 0$ (fig. 2) or $|\phi_s(\omega)| < 90^0$ (not shown). This peak is absent in $(K^+\omega)$. The fits described in sect. 3.2 suggest this peak to be mostly due to a state with $J^P = 2^-$, with cross section larger in K^-p than in K^+p reactions. A Deck mechanism similar to that described above for the (Kω) mass region 1.4 - 1.6 GeV may be at work also here, with possible resonance production by final state interaction.

6. CONCLUSIONS

The (Kω) systems produced in the reactions $K^\pm p \to (K^\pm\omega)p$ have been investigated, for (Kω) masses from threshold up to 2 GeV, using two K^+ experiments at 8.25 and 16 GeV/c, and two K^- experiments at 10 and 16 GeV/c.

Studies of mass spectra, t distributions, energy dependence of the cross sections, moments of the decay angular distributions, as well as partial wave analyses have produced the following results:

(i) In both K^+p and K^-p interactions, the (Kω) mass spectrum shows a strong threshold enhancement. At higher masses, a second enhancement at ∿ 1.7 GeV is seen with incident K^-, but is not evident with K^+.

(ii) The threshold enhancement (M(Kω) < 1.35 GeV) is found to be similar in K^+ and K^- induced reactions. In both cases it peaks closer to threshold than the enhancement observed in the mass

spectrum of the ($K\pi\pi$) system. Its energy dependence is found to be very weak, specially for K^-. A partial wave analysis shows that the states $J^P LM\eta = 0^-P0+$, 1^+S0+ and 1^+S1+ are sufficient to describe this mass region, that the 1^+ states are largely dominant and that they are produced by a mechanism which conserves s channel helicity.

The properties observed here for the ($K\omega$) system are very similar to those reported for the system ($K\rho$), where the threshold enhancement in the 1^+ state has been interpreted as a decay mode of a diffractively produced resonance, $Q_1(1290)$. It is therefore suggested that the threshold enhancement in the 1^+S state of the ($K\omega$) system corresponds to another decay mode of the same resonance.

The ratio of the coupling constants of Q_1 to the $K\omega$ and $K\rho$ decay channels, $R_\omega = g^2_{K\omega}/g^2_{K\rho}$, is determined to be 0.21 ± 0.04. This value is consistent with the SU(3) classification of the 1^+ multiplet.

(iii) In the ($K\omega$) mass region 1.4 - 1.6 GeV, the states $J^P = 2^+D$ becomes important besides 0^-P and 1^+S. Here, remarkable differences are found between ($K^-\omega$) and ($K^+\omega$) data namely a much stronger contribution of 1^+S1+ (and less 0^-P0+) is present with K^- than with K^+. A study of the events in this mass region in terms of ϕ_s, the azimuthal angle of the ω in the s channel helicity system, indicates that the production processes involved are predominantly of the Deck type.

The relatively large amount of 0^-P found in the analysis is consistent with the observation that the t' distribution for this mass region show no indication of flattening near $t' = 0$.

(iv) Above 1.6 GeV, in the L region, the state $J^P = 2^-$ begins to contribute and becomes dominant, with its maximum at $\sim$ 1.7 GeV. Here, again, K^+ and K^- interactions are different, the 2^- state having a cross section $\sim$ 1.5 times larger in K^- than in K^+.

Possibly, a Deck mechanism similar to that operating in the 1.4 - 1.6 GeV region is at work also here. This justifies the facts that the enhancement at $\sim$ 1.7 GeV is seen almost exclusively in K^- interactions and that the amplitude of the signal decreases rapidly with increasing energy as expected for Reggeon exchange processes. It is important to remark that the $J^P = 2^-$ state alone is not sufficient to describe the enhancement observed in the L region, which therefore cannot be a pure resonant state.

In conclusion, the production of ($K\omega$) systems with masses less than 2 GeV in the reactions $K^{\pm}p \to K^{\pm}\omega p$ contains diffractive components which, at low masses, are basically similar for K^+ and K^- and are dominated by the Q_1 resonance. With increasing mass, non-diffractive exchange mechanisms start contributing, generating differences between the K^+ and K^- induced reactions. The excess of ($K^-\omega$) over ($K^+\omega$) production can be interpreted in the framework of the Deck model by non-exotic virtual K^-p scattering being favoured over exotic K^+p scattering.

APPENDIX

PARTIAL WIDTHS AND COUPLING CONSTANTS OF THE $Q_1(1290)$ DECAY CHANNELS

In the determination of partial widths and branching ratios for the various decay modes of the $Q_1(1290)$ resonance there are not only statistical limitations, but also conceptual problems. In fact, its decay channels are numerous ($K\rho$, $K\omega$, $K^*(890)\pi$, $\kappa\pi$ and $K\varepsilon$) and all have thresholds close to the resonance mass. The number of events found in each of these final states is consequently strongly influenced by phase-space effects which distort the shape of the mass distributions. The situation is further complicated by the fact that ρ and ω have different and not negligible width. As discussed by Dunwoodie and Lasinski [15], it is preferable to determine, instead of branching ratios, the relative coupling constants of Q_1 to the various decay channels, as these are less critically dependent on the exact knowledge of the resonance parameters. The coupling constant, g_i for a given decay channel is related to the partial width Γ_i at the resonance mass M_0 by

$$\Gamma_i = \frac{\langle Q \rangle}{M_0^2} \, g_i^2$$

where $\langle Q \rangle$ is a suitably defined average decay momentum.

A simplified solution to this problem was presented in ref. [15] and was discussed together with alternative solutions in ref. [17]. Here we propose a solution which treats all decay channels simultaneously by defining a mass dependent total width. In this way one arrives at a more coherent picture on how the opening up of a new channel modifies the other channels.

In the following formulation of a mass dependent width we will make the basic assumption that the total width is proportional to the total available phase space, suitably modified to allow for the centrifugal-barrier effect of angular momentum. This implies summing over all decay channels and taking into account the probability for the formation of an intermediate resonance which again will depend on the available phase space. For simplicity all decays are treated as two-body decays, $\omega \to 3\pi$ being approximated by $\omega \to (2\pi) + \pi$. We then get

$$\Gamma(M) = \sum_i \Gamma_i(M) \qquad \text{(A1)}$$

with $$\Gamma_i(M) = \int_{thr}^{M-m_i} \Gamma_i(M,m)\,dm$$

and $$\Gamma_i(M,m) = \Gamma_0 \frac{g_i^2}{M_0} \left[\frac{Q_i(M,m)}{M}\right]^{2L+1} f_i(m) \Big/ \sum_i \frac{g_i^2}{M_0} \int_{thr}^{M_0-m_i} \left[\frac{Q_i(M,m)}{M_0}\right]^{2L+1} f_i(m)\,dm,$$

where

M = mass of Q_1

m = mass of daughter resonance

m_i = mass of the pseudoscalar meson in decay channel i

g_i = coupling constant of decay channel i

Q_i = relative decay momentum

L = relative decay angular momentum

f_i = normalized Breit-Wigner distribution for daughter resonance i (see below).

The denominator of $\Gamma_i(M,m)$ in eq. (A1) has been chosen such that

$$\Gamma(M_0) = \sum_i \Gamma_i(M_0) = \sum_i \int_{thr}^{M_0-m_i} \Gamma_i(M,m)\,dm = \Gamma_0 \ .$$

The Breit-Wigner distributions for the parent and the daughter resonances are defined as

$$BW_i(M) = \frac{M\,M_0\,\Gamma_i(M)}{(M_0^2 - M^2)^2 + M_0^2\,\Gamma_{tot}^2(M)} \qquad \text{(A2)}$$

and

$$BW_i(m) = \frac{m\,m_0\,\gamma_i(m)}{(m_0^2 - m^2)^2 + m_0^2\,\gamma_i^2(m)} \ ,$$

with $\gamma_i(m) = \gamma_i(m_0) \left(\frac{q}{m} \cdot \frac{m_0}{q_0}\right)^{2\ell+1}$ and q and ℓ the relative decay momentum and angular momentum of the daughter resonance (note that the threshold

factor q^{ℓ} has been replaced by $(\frac{q}{m})^{\ell}$, which makes little difference at threshold, but stops the integral of BW(m) from diverging at large masses).

The normalization of $BW_i(m)$ (discussed in ref. [17]) is

$$f_i(m) = BW_i(m) \Big/ \int_{thr}^{\infty} BW_i(m)\, dm.$$

In view of the basic assumption that the width is proportional to the available phase space, the normalization is made to the "undistorted phase space" [17], i.e. to the complete integral of the BW distribution. Normalising to the so-called "physical phase space", i.e. integrating from threshold to $(M - m_i)$, would in fact eliminate this proportionality, to first order.

To apply the formalism outlined above to the decay of the Q_1 we use as constraints the shape of the mass spectrum of the $Q^+ \to K^+\rho$ channel, the amount of $(K\varepsilon + K\pi)$ relative to $K\rho$ as determined in the SLAC counter experiment [2] and the amount of $K\omega$ relative to $K\rho$ determined in this experiment. Neglecting the decay of $K^*(890)\pi$ which is found to be small [2], we thus try to find the parameters M_0, Γ_0, $R_\omega = g^2_{K\omega}/g^2_{K\rho}$ and $R_{\varepsilon+\kappa} = g^2_{(K\varepsilon+K\pi)}/g^2_{K\rho}$ which describe the data. As the integration in eq. (A1) can only be done numerically, an actual least square fit to the data is too time consuming. Instead, mass plots for $K\rho$, $K\omega$ and $(K\varepsilon + K\pi)$ have been calculated for many different sets of parameters and compared to the data.

A good description of the data (fig. A1) has been obtained with $M_0 = 1.30$ GeV, $\Gamma_0 = 0.18$ GeV, $R_\omega = 0.21$ and $R_\varepsilon = 12$. The values of M_0 and Γ_0 are essentially determined by the shape of the $K\rho$ mass spectrum and depend only weakly on the values of R_ω and R_ε. The error on R_ω has been determined to be 0.04 corresponding to the 1 std limits of $\sigma(K^-\omega)$ at fixed values of M_0, Γ_0 and R_ε. The value of R_ε is large because in the definition of g_i^2 (eq. (A1)), a normalisation factor of $(M_0/Q_0)^2$, necessary for P waves, has been included into g_i^2 for simplicity. Note that the $K\rho$ final state peaks at 1.27 GeV, i.e. 30 MeV below the nominal resonance mass. This is understandable qualitatively for a total width increasing with mass [20]. Forgetting the mass dependence in the numerator, one obtains the minimum of the BW denominator when

$$M^2 - M_0{}^2 + M_0{}^2 \, \Gamma \left. \frac{d\Gamma}{dM^2} \right|_{M^2} = 0.$$

Approximating the mass dependence of the width near M_0 by a linear expression in M : $\Gamma = \Gamma_0 + a(M-M_0)$ results in

$$M = M_0 - \frac{a\Gamma_0}{4 + a^2} \quad .$$

The maximum of the distribution is therefore shifted to a mass smaller than M_0 by an amount depending on $d\Gamma/dM^2\big|_{M_0}$. In fig. A1, $\Gamma_{tot}(M)$ is shown for the optimal parameters. It turns out that the parameter a is close to 2, independent of $R_{\varepsilon+K}$, which gives, in this approximation, a maximum shift of $\Gamma/4$.

As long as the detailed line shape of the Kω final state is not known, the width depends entirely on the Kρ line shape, i.e. essentially on the ratio of the Kρ cross section at M = 1.5 GeV to its peak value. The rise at the low mass side adds little information on the width, as it is determined by the threshold behaviour. This rise is, however, quite sensitive to the value of the resonance mass M_0 which - in our parametrization - is determined to better than 10 MeV.

REFERENCES

[1] Aachen-Berlin-CERN-London-Vienna Collaboration, G. Otter et al., Nucl. Phys. B106 (1976) 77.

[2] G.W. Brandenburg et al., Phys. Rev. Lett. 36 (1976) 703, 706 and 1239.

[3] R.K. Carnegie et al., Phys. Lett. 63B (1976) 235.

[4] A. Barbaro-Galtieri et al., Phys. Rev. Lett. 22 (1969) 1207; Aachen-Berlin-CERN-London-Vienna Collaboration, J. Bartsch et al., Phys. Lett. 33B (1970) 186.

[5] Data on the reaction $K^+p \to K^+\omega p$ have been published at the following incident momenta:

4.6 and 9 GeV/c: G. Alexander et al., Phys. Rev. 177 (1969) 2092;
6.8 GeV/c: C.Y. Chien et al., Nucl. Phys. B104 (1976) 189;
10 GeV/c: D.C. Colley et al., Nucl. Phys. B26 (1971) 71;
12 GeV/c: P.J. Davies et al., Nucl. Phys. B44 (1973) 344;

and on $K^-p \to K^-\omega p$ at:

3.8 GeV/c: D.D. Carmony et al., Phys. Rev. Lett. 18 (1967) 615;
6 GeV/c: R.E. Juhala et al., Phys. Rev. 84 (1969) 1461;
8.25 GeV/c: P. Theocharopoulos et al., Nucl. Phys. B83 (1974) 1.

and at 7.3 GeV/c [7] and 10 GeV/c [8].

[6] Aachen-Berlin-CERN-London-Vienna Collaboration, J.Bartsch et al., Phys. Lett. 22B (1966) 357.

[7] S.U. Chung et al., Phys. Lett. 51B (1974) 413.

[8] Aachen-Berlin-Bonn-CERN-Heidelberg-London-Vienna Collaboration, G. Otter et al., Nucl. Phys. B87 (1975) 189.

[9] Aachen-Berlin-Bonn-CERN-Heidelberg-London-Vienna Collaboration, P. Bosetti et al., Nucl. Phys. B101 (1975) 304.

[10] Brussels-CERN-Mons-Serpukhov Collaboration, D. Johnson et al., Nucl. Phys. B115 (1976) 195.

[11] S.U. Chung, Phys. Rev. 169 (1968) 1342.

[12] G. Ascoli et al., Phys. Rev. Lett. 25 (1970) 962.

[13] J.D. Hansen et al., Nucl. Phys. B81 (1974) 403.

REFERENCES (Cond't)

[14] R.K. Carnegie et al., Nucl. Phys. B127 (1977) 509.

[15] W. Dunwoodie and T. Lasinski, SLAC Group B Physics Memo (1976).

[16] R.K. Carnegie et al., Phys Lett. 68B (1977) 287.

[17] M. Mazzucato et al., Nucl. Phys. B156 (1979) 532.

[18] E.L. Berger, Phys. Rev. D11 (1975) 3214 and in "Three-particle Phase Shift Analysis and Meson Resonance Production". Daresbury Study Week-end No. 8, February 1975, Proceedings edited by J.B. Dainton and A.J.G. Hey.

[19] Aachen-Berlin-Bonn-CERN-Heidelberg Collaboration, P. Bosetti et al., Nucl. Phys. B103 (1976) 189.

[20] J.D. Jackson, Nuovo Cim. 34 (1964) 1644.

TABLE CAPTIONS

Table 1 Number of events of the reactions $K^{\pm}p \to K^{\pm}\pi^{+}\pi^{-}\pi^{o}p$ and number of events and cross sections for the channels $K^{\pm}p \to (K^{\pm}\omega)p$.

Table 2 Spin-parity decomposition of $(K^{\pm}\omega)$ systems close to threshold ($1.28 < M(K\omega) < 1.35$ GeV) and density matrix elements of the $1^{+}S$ state.

Table 3 Spin-parity decomposition for $(K^{\pm}\omega)$ systems with masses between 1.3 and 2.0 GeV.

TABLE 1

	K^+p		K^-p	
	8.25 GeV/c	16 GeV/c	10 GeV/c	16 GeV/c
Number of events fitting $K^{\pm}p \to K^{\pm}\pi^+\pi^-\pi^0 p$	6840	15 064	11 824	14 613
Number of events fitting $Kp \to K\omega p$	265	494	389	450
nb/event	145 ± 10	47.5 ± 3.5	82 ± 4	55.5 ± 3
$\sigma(Kp \to K\omega p)$ (μb)	39.2 ± 3.6	22.1 ± 1.9	33.0 ± 2.3	28.3 ± 1.9

TABLE 2

	$Kp \to (K\omega)p$		$1.28 < M(K\omega) < 1.35$ GeV	
	K^+p (8.25 + 16 GeV/c)		K^-p (10 + 16 GeV/c)	
Number of events	110		113	
0^-P	15 ± 15		17 ± 10	
1^+S	95 ± 15		96 ± 10	
	Density matrix elements of the 1^+S state			
	GJ	H	GJ	H
ρ_{00}	0.60 ± 0.11	0.78 ± 0.12	0.75 ± 0.13	0.97 ± 0.14
ρ_{11+}	0.40 ± 0.12	0.22 ± 0.11	0.25 ± 0.12	0.03 ± 0.13
$Re\rho_{01+}$	-0.24 ± 0.08	0.06 ± 0.08	-0.43 ± 0.07	0.04 ± 0.08

TABLE 3

	$K^+p \to (K^+\omega)p$					
Mass interval (GeV)	1.3-1.5	1.4-1.6	1.5-1.7	1.6-1.8	1.7-1.9	1.8-2.0
Number of events	276	246	220	191	166	124
0^-P0+	75±17	70±18	51±15	13±13	15±12	4±16
1^+S0+	78±14	66±14	65±17	19±20	19±18	18±15
1^+S1+	51±19	29±21	12±19	32±12	26±11	22±11
2^-P0+		0±10	19±10	18± 9	16± 8	6± 5
2^-F0+		14±17	16±10	36±13	36±13	38±13
2^+D1+	24±14	22±13	33±13			
2^+D0-	48±12	45±12	25±11			
3^-F1+				33±10	33± 9	22± 8
3^-F0-				40±15	20±14	14±13
3^+D0+						
total 0^-	75±17	70±18	51±15	13±13	15±12	4±16
1^+	129±26	95±27	77±26	51±26	46±22	40±20
2^-		14±17	34±14	54±14	52±14	44±13
2^+	72±17	67±18	57±18			
3^-				33±10	33± 9	22± 8
3^+				40±15	20±14	14±13

	$K^-p \to (K^-\omega)p$					
1.3-1.5	1.4-1.6	1.5-1.7	1.6-1.8	1.7-1.9	1.8-2.0
320	246	216	219	192	139
57±17	41±22	42±17	17±15	27±14	12±13
122±17	49±15	54±20	36±22	19±18	9±15
91±18	103±22	55±19	53±19	41±18	25±16
	2± 3	7± 7	36±11	48±10	63±13
	17±14	15±12	51±11	34±10	3± 3
33±14	17±14	28±14			
22±10	16±10	16± 9			
			12±12	12±13	11±11
			13± 9	13± 8	15± 8
52±17	41±22	42±17	17±15	27±14	12±13
213±27	152±30	108±30	89±27	60±23	34±22
	19±16	22±18	88±21	82±14	66±13
55±17	33±17	44±17			
			25±15	24±16	27±13

FIGURE CAPTIONS

Fig. 1 ($K\omega$) mass spectra in the reactions $K^{\pm}p \to (K^{\pm}\omega)p$ at various energies. The ω is defined by the following mass cuts:

K^+p at 8.25 and 16 GeV/c, and K^-p at 10 and 16 GeV/c (this work): $0.76 < M(3\pi) < 0.81$ GeV;

K^+p at 10 GeV/c (private communication): $0.74 < M(3\pi) < 0.83$ GeV;

K^-p at 7.3 GeV [7]: $0.743 < M(3\pi) < 0.823$ GeV.

Fig. 2 ($K\omega$) mass spectra for events with ω going backward or forward in the Gottfried-Jackson system of the ($K\omega$) rest frame.

Fig. 3 Energy dependence of the cross section for the channels $K^{\pm}p \to (K^{\pm}\omega)p$.

Fig. 4 The exponent n of $\sigma \propto p_{lab}^{n}$ measuring the energy dependence of the ($K\omega$) production cross section as a function of the ($K\omega$) mass. Data at 8.25, 10, 12 and 16 GeV/c are used for K^+p reactions and at 7.3, 10 and 16 GeV/c for K^-p reactions.

Fig. 5 $d\sigma/dt'$ distributions for the production of ($K\omega$) systems for several intervals of the ($K\omega$) mass. The data of our four experiments (K^+p at 8.25 and 16 GeV/c and K^-p at 10 and 16 GeV/c) have been combined. The solid lines are fits with $\exp(-Bt')$ for $t' > 0.05$ GeV^2 and the values of B are indicated.

Fig. 6 Normalized moments $H(LM,\ell m)$ of the ω angular distribution as functions of the ($K\omega$) mass. Crosses indicate results of maximum likelihood fits to the data in overlapping mass intervals, 200 MeV wide. They should, therefore, describe the average of two neighbouring data points.

Fig. 7 The moments combinations Σ_0 and Σ_1 measuring the ω helicity as defined in formula (6), as functions of the ($K\omega$) mass.

FIGURE CAPTIONS (Condt'd)

Fig. 8 Mass distribution and spin-parity decomposition of the (Kω) systems for the combined data of all four experiments.

Fig. 9 Distributions of ϕ_s, the azimuthal angle of the ω in the s channel helicity system, for (Kω) masses between 1.4 and 1.6 GeV, and double exchange diagrams for the reactions $K^{\pm}p \to K^{\pm}\omega p$.

Fig. A1 (Appendix)
Mass spectrum of the 1^+ state of the (Kρ) system and total width of the 1^+ state calculated from eq. (A1) using the values of the parameters M_0, Γ_0, R_ω and $R_{\varepsilon+K}$ given in the text. The shape of the (Kρ) mass spectrum is compared with the experimental results (crosses) of the SLAC experiment of ref. [2].

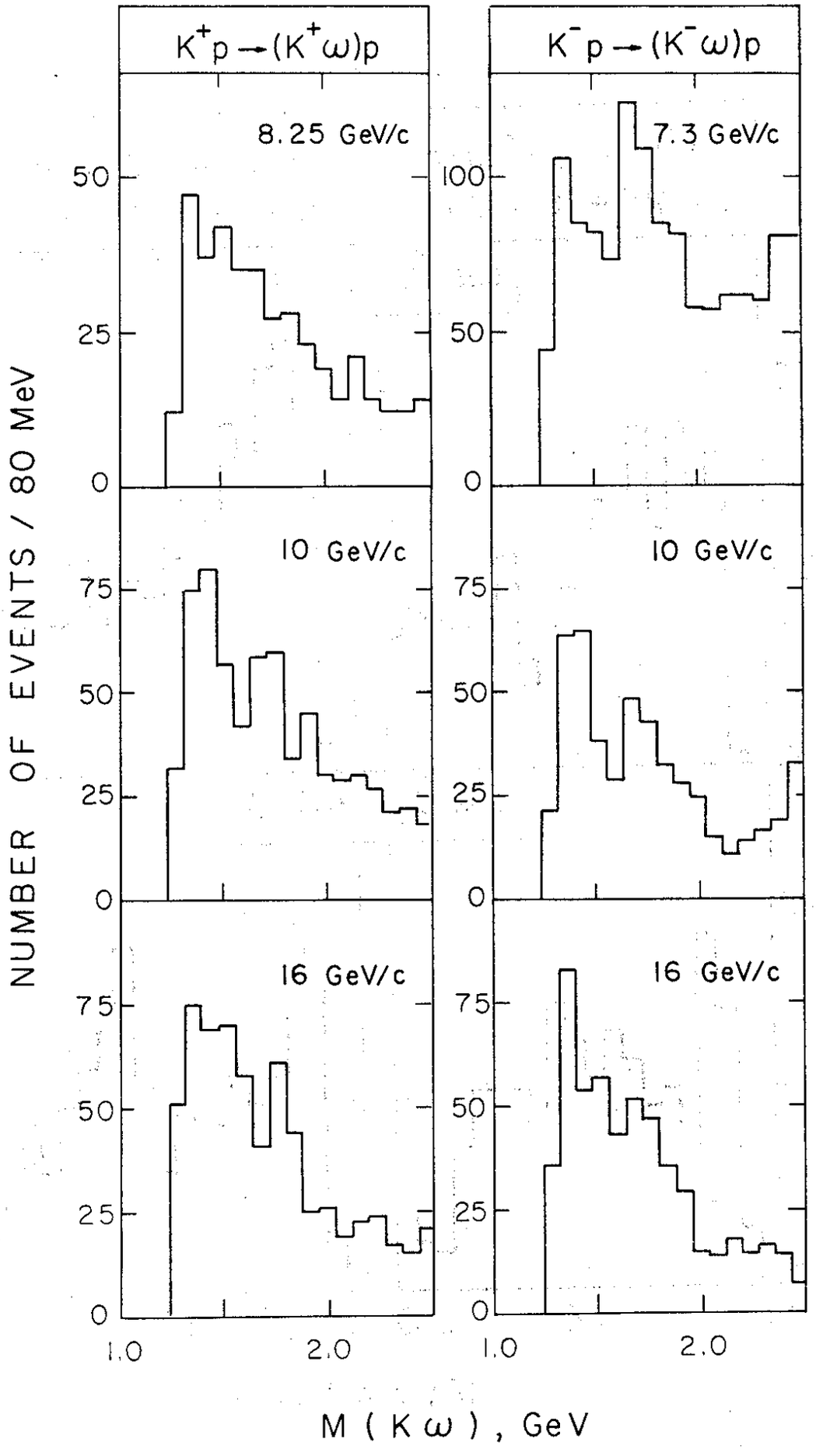
$K^+p \rightarrow (K^+\omega)p$
$K^-p \rightarrow (K^-\omega)p$
8.25 GeV/c
7.3 GeV/c
10 GeV/c
10 GeV/c
16 GeV/c
16 GeV/c
NUMBER OF EVENTS / 80 MeV
M (K ω) , GeV
0
25
50
75
100
1.0
2.0

Fig. 1

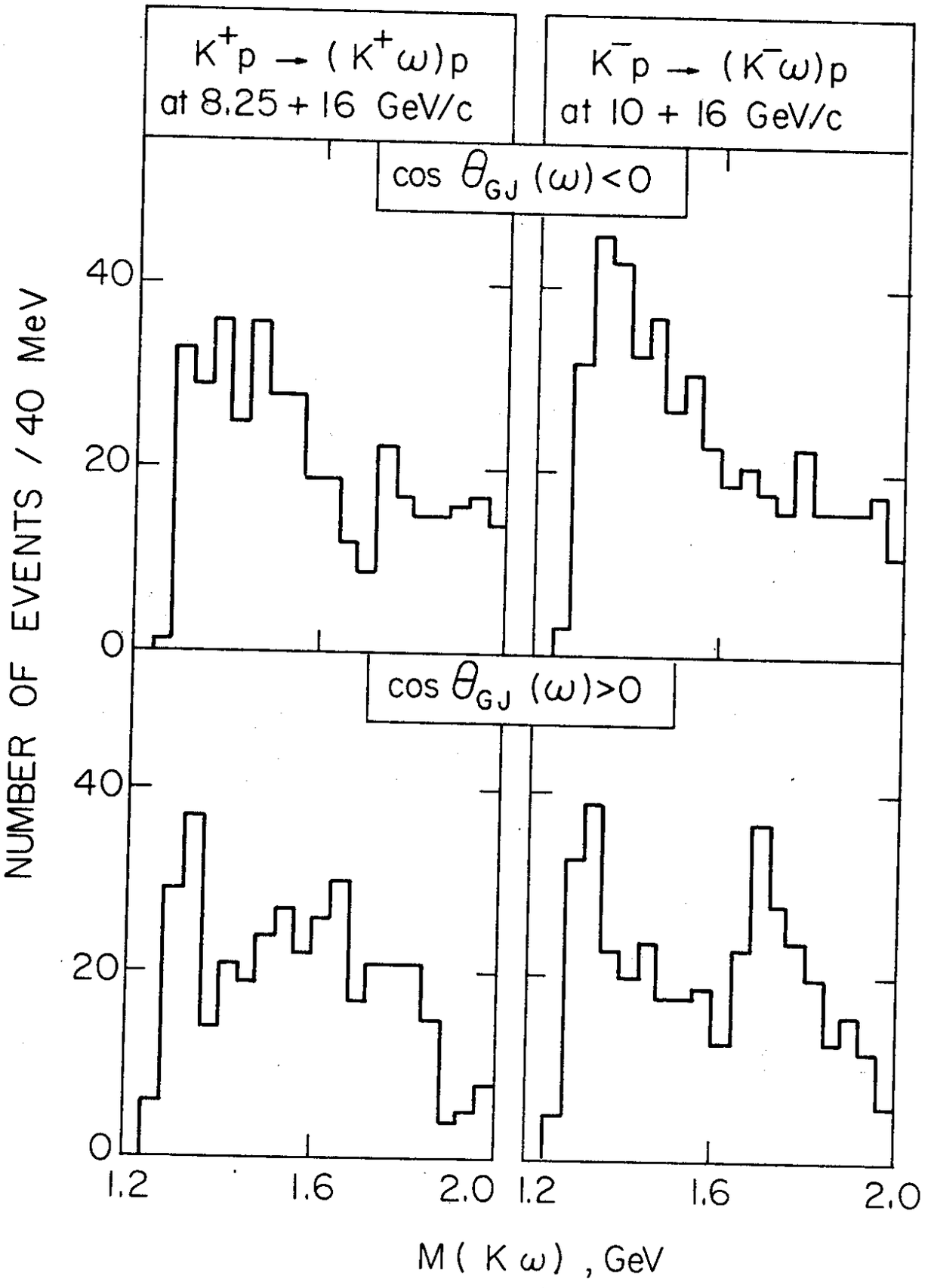
$K^+p \rightarrow (K^+\omega)p$
at 8.25 + 16 GeV/c
$K^-p \rightarrow (K^-\omega)p$
at 10 + 16 GeV/c
$\cos\theta_{GJ}(\omega)<0$
$\cos\theta_{GJ}(\omega)>0$
NUMBER OF EVENTS / 40 MeV
0
20
40
1.2
1.6
2.0
M(K ω) , GeV

Fig. 2

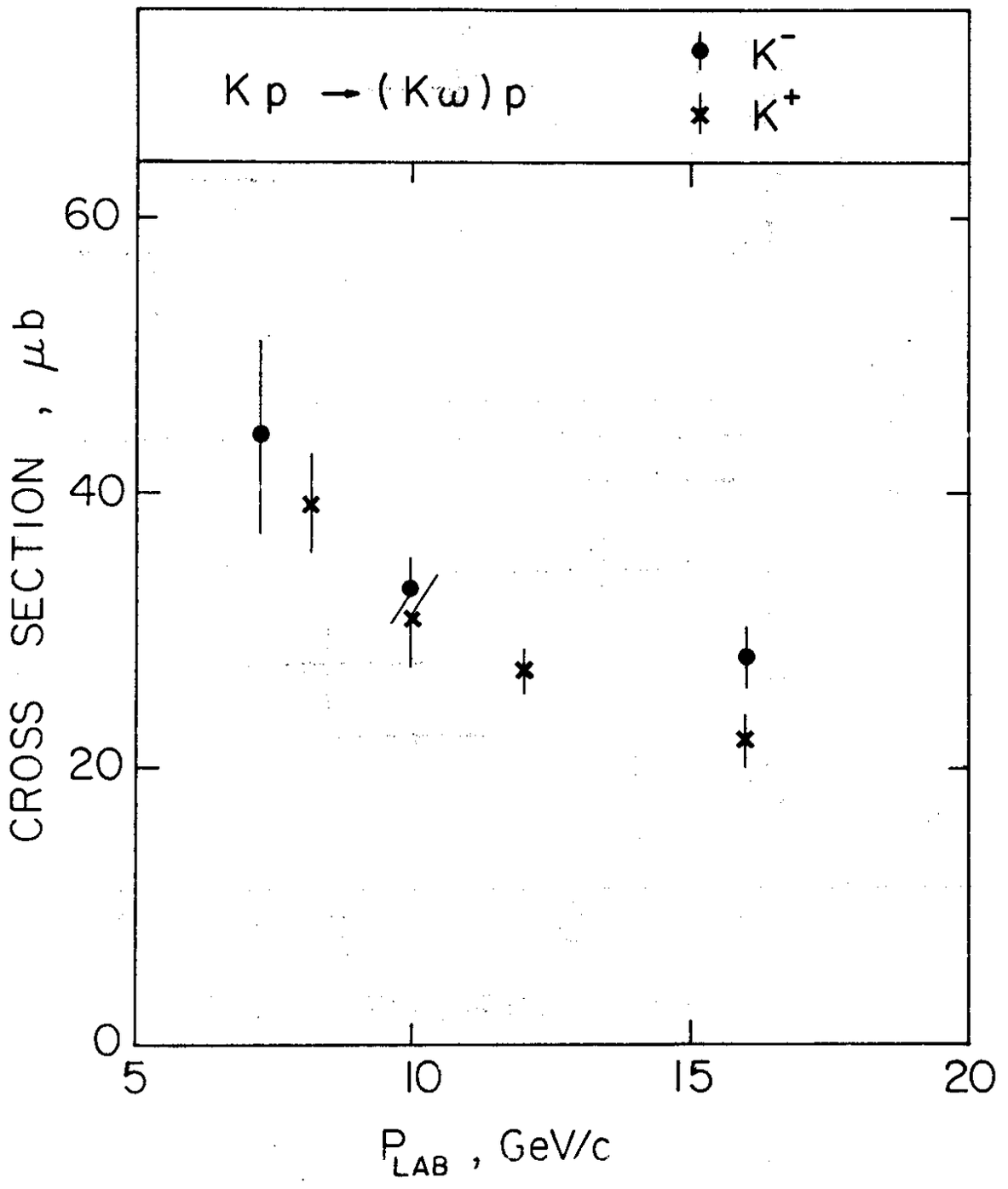

Fig. 3

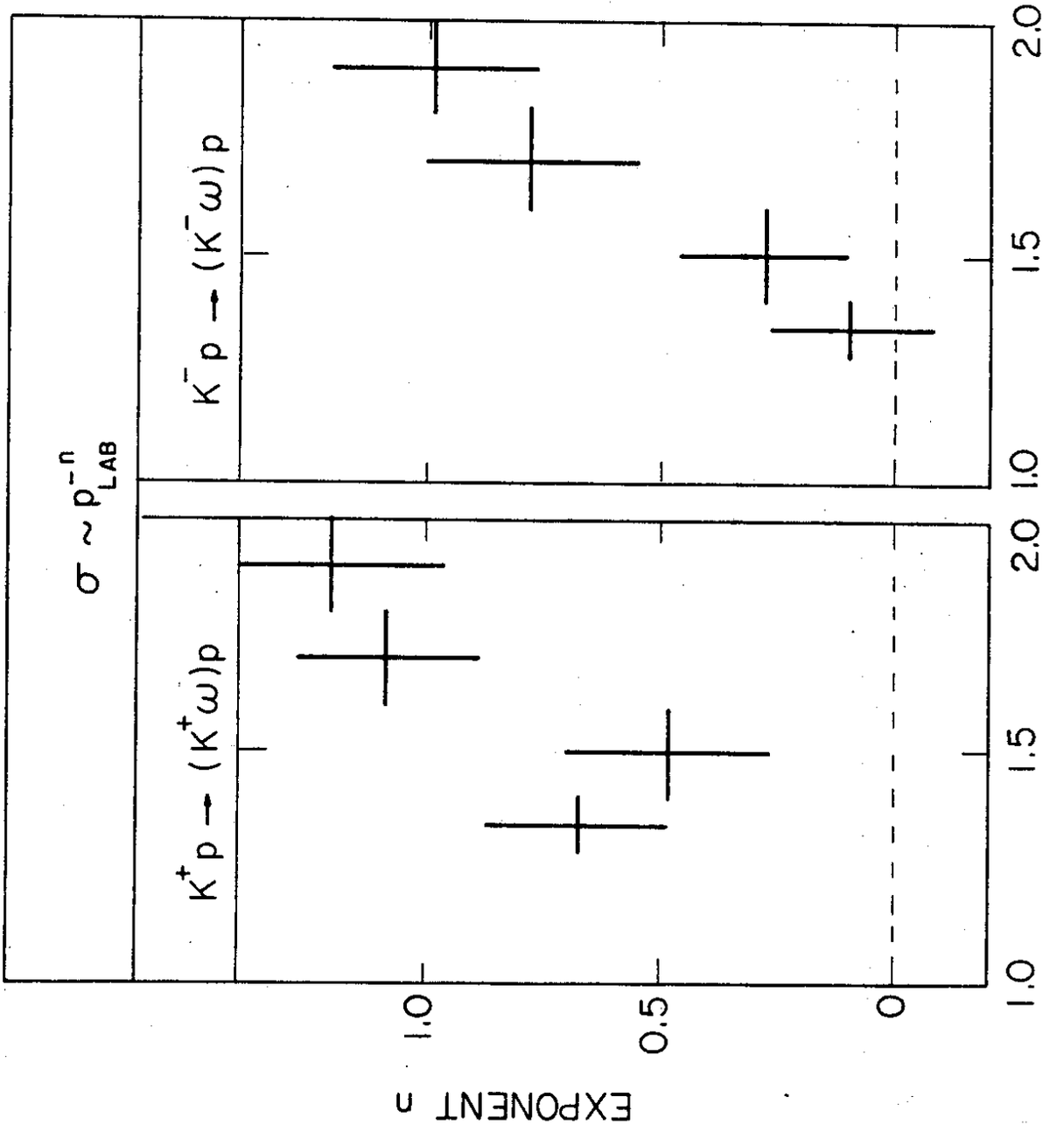
$\sigma \sim p_{LAB}^{-n}$
$K^+ p \to (K^+\omega) p$
$K^- p \to (K^-\omega) p$
EXPONENT n
1.0
0.5
0
1.0
1.5
2.0
1.0
1.5
2.0
M(Kω), GeV

Fig. 4

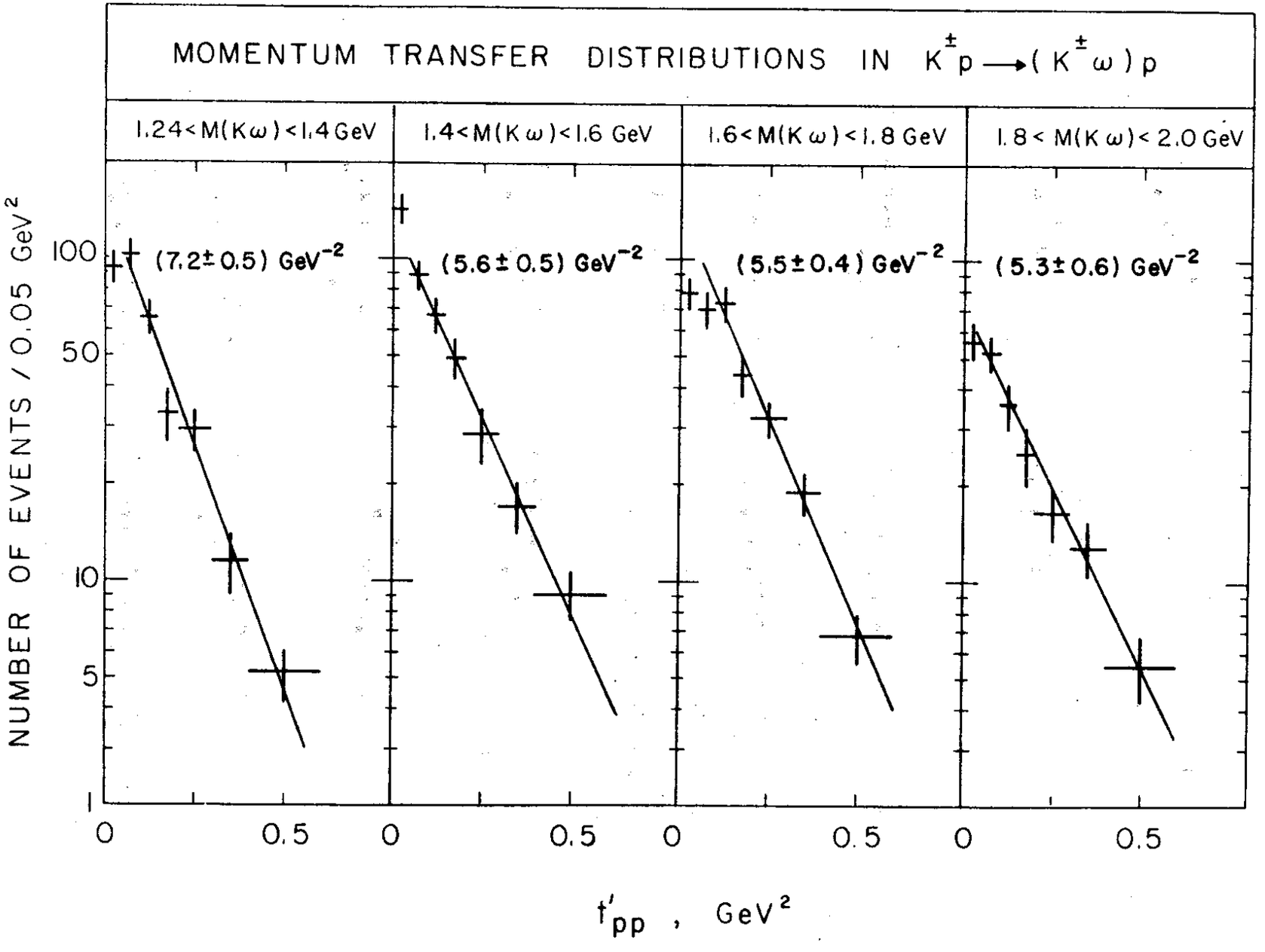
MOMENTUM TRANSFER DISTRIBUTIONS IN $K^{\pm}p \longrightarrow (K^{\pm}\omega)p$
1.24<M(Kω)<1.4 GeV
1.4<M(Kω)<1.6 GeV
1.6<M(Kω)<1.8 GeV
1.8<M(Kω)<2.0 GeV
(7.2±0.5) GeV^{-2}
(5.6±0.5) GeV^{-2}
(5.5±0.4) GeV^{-2}
(5.3±0.6) GeV^{-2}
NUMBER OF EVENTS / 0.05 GeV^2
100
50
10
5
1
0
0.5
t'_{pp} , GeV^2

Fig. 5

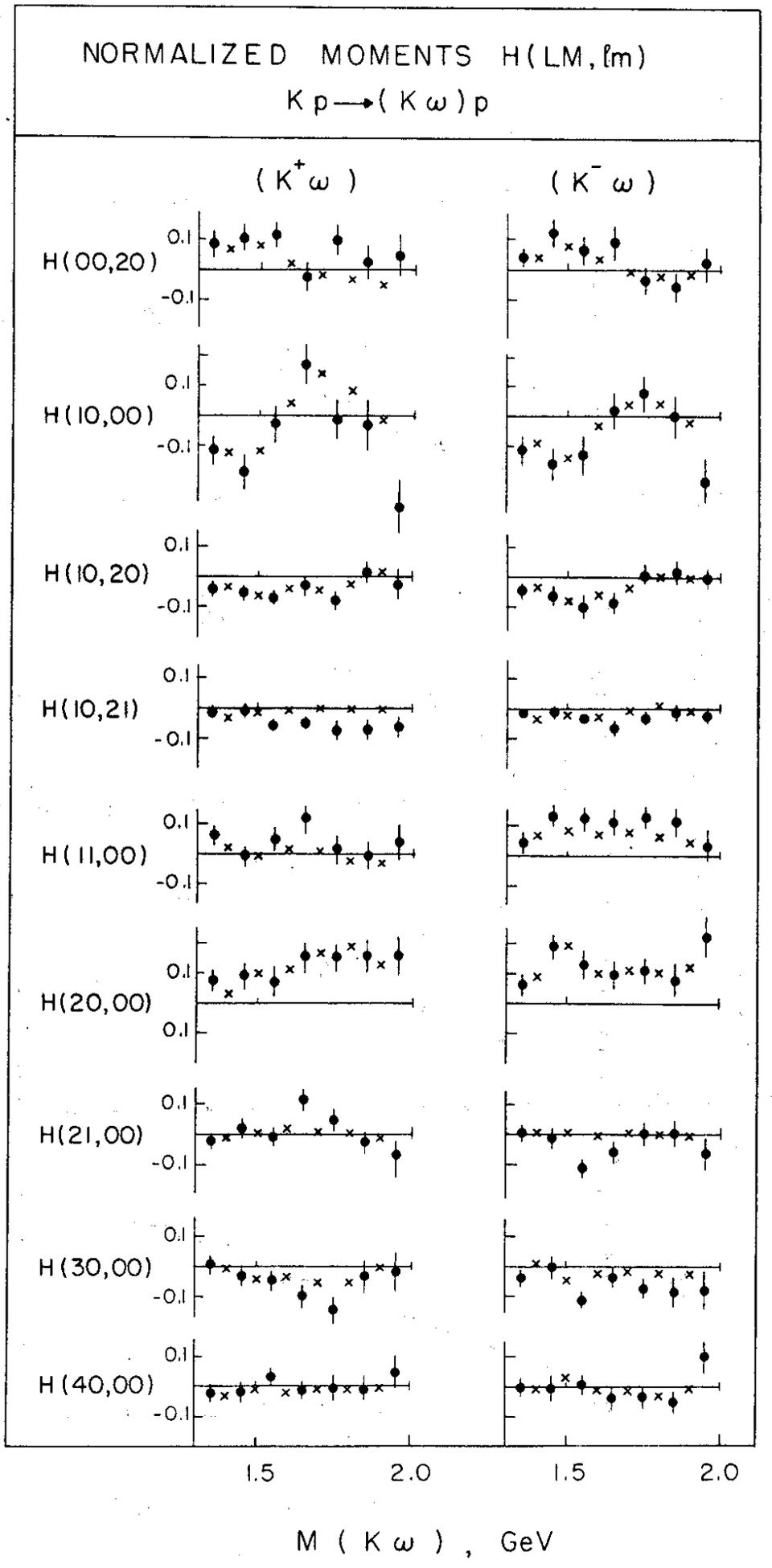
NORMALIZED MOMENTS H(LM, ℓm)
K p ⟶ (K ω) p
(K⁺ ω)
(K⁻ ω)
H(00,20)
H(10,00)
H(10,20)
H(10,21)
H(11,00)
H(20,00)
H(21,00)
H(30,00)
H(40,00)
0.1
-0.1
1.5
2.0
M (K ω) , GeV

Fig. 6

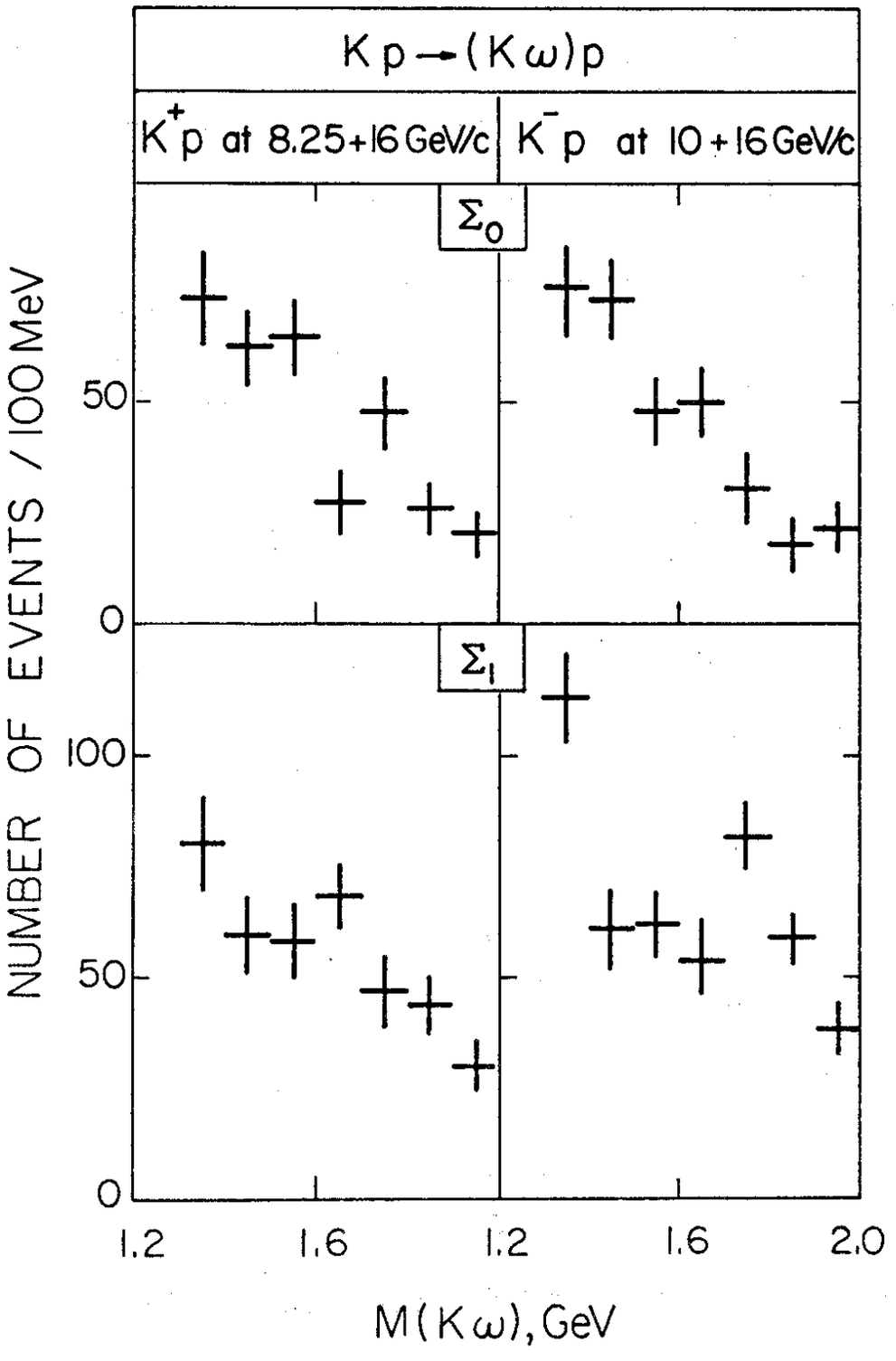
K p → (K ω) p
K⁺ p at 8.25+16 GeV/c
K⁻ p at 10+16 GeV/c
Σ0
Σ1
NUMBER OF EVENTS / 100 MeV
50
0
100
50
0
1.2
1.6
1.2
1.6
2.0
M(K ω), GeV

Fig. 7

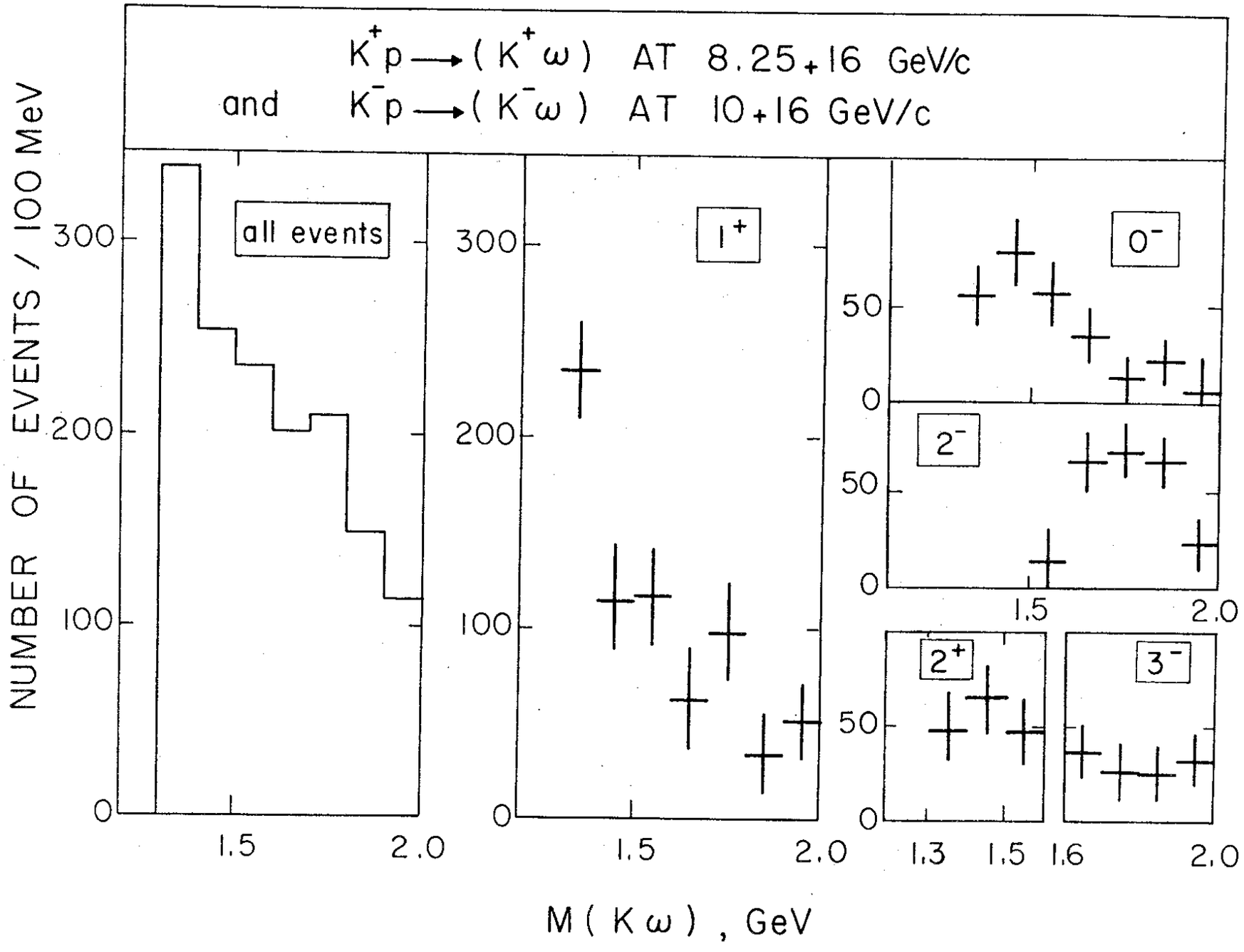
$K^+p \rightarrow (K^+\omega)$ AT 8.25+16 GeV/c
and $K^-p \rightarrow (K^-\omega)$ AT 10+16 GeV/c
all events
1^+
0^-
2^-
2^+
3^-
NUMBER OF EVENTS / 100 MeV
M (K ω) , GeV

Fig. 8

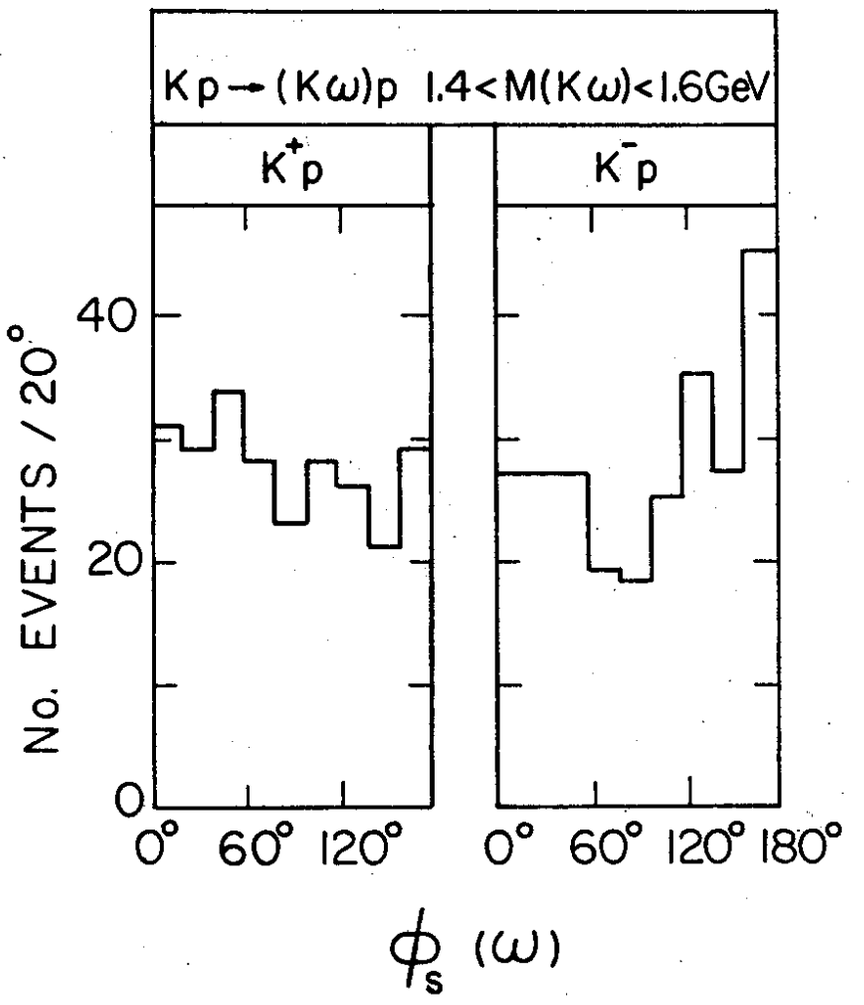
Kp → (Kω)p 1.4<M(Kω)<1.6GeV
K⁺p
K⁻p
No. EVENTS / 20°
40
20
0
0° 60° 120°
0° 60° 120° 180°
φs (ω)

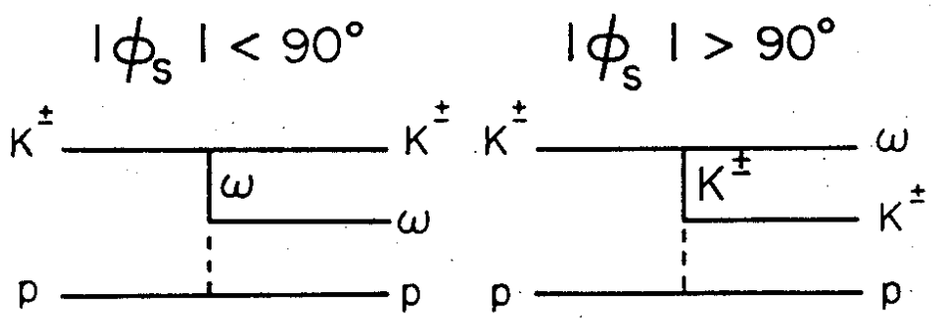
|φs| < 90°
|φs| > 90°
K±
K±
ω
ω
p
p
K±
ω
K±
K±
p
p

Fig. 9

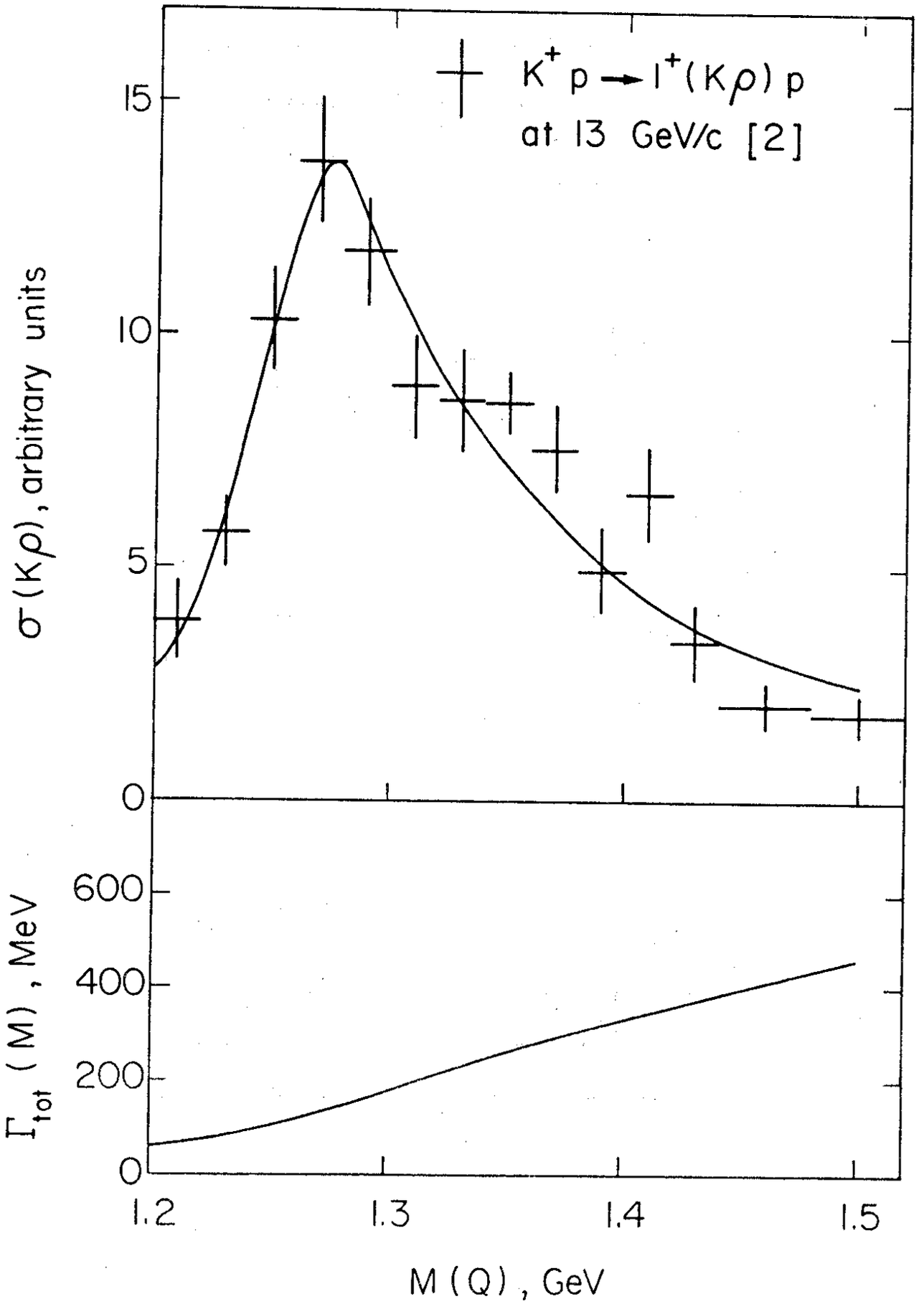
$K^+ p \rightarrow l^+ (K\rho) p$
at 13 GeV/c [2]
$\sigma(K\rho)$, arbitrary units
15
10
5
0
$\Gamma_{tot}(M)$, MeV
600
400
200
0
1.2
1.3
1.4
1.5
M(Q), GeV

Fig. A1